

See discussions, stats, and author profiles for this publication at: <https://www.researchgate.net/publication/229887649>

# Forecast of daily mean, maximum and minimum temperature time series by three artificial neural network methods

Article in *Meteorological Applications* · December 2008

DOI: 10.1002/met.83

CITATIONS

138

READS

3,973

3 authors, including:



Beyza Ustaoglu  
Sakarya University

36 PUBLICATIONS 390 CITATIONS

[SEE PROFILE](#)



Mehmet Karaca  
Istanbul Technical University

72 PUBLICATIONS 2,351 CITATIONS

[SEE PROFILE](#)

# Forecast of daily mean, maximum and minimum temperature time series by three artificial neural network methods

B. Ustaoglu,<sup>a\*</sup> H. K. Cigizoglu<sup>b</sup> and M. Karaca<sup>a,c</sup>

<sup>a</sup> *Eurasia Institute of Earth Sciences, Istanbul Technical University, 34469 Maslak, Istanbul, Turkey*

<sup>b</sup> *Civil Engineering Faculty, Hydraulics Division, Istanbul Technical University, 34469 Maslak, Istanbul, Turkey*

<sup>c</sup> *Faculty of Mining, Department of Geology, Istanbul Technical University, 34469 Maslak, Istanbul, Turkey*

**ABSTRACT:** Temperature forecasting has been one of the most important factors considered in climate impact studies on sectors of agriculture, vegetation, water resources and tourism. The main purpose of this study is to forecast daily mean, maximum and minimum temperature time series employing three different artificial neural network (ANN) methods and provide the best-fit prediction with the observed actual data using ANN algorithms.

The geographical location considered is one of Turkey's most important areas of agricultural production, the Geyve and Sakarya basin, located in the south-east of the Marmara region (40°N and 30°E). The methods chosen in this study are: (1) feed-forward back propagation (FFBP), (2) radial basis function (RBF) and, (3) generalized regression neural network (GRNN). Additionally, predictions with a multiple linear regression (MLR) model were compared to those of the ANN methods. All three different ANN methods provide satisfactory predictions in terms of the selected performance criteria; correlation coefficient (*R*), root mean square error (RMSE), index of agreement (IA) and the results compared well with the conventional MLR method. Copyright © 2008 Royal Meteorological Society

**KEY WORDS** feed-forward back propagation; radial basis function; generalized regression neural network; multiple linear regression; daily temperature time series

*Received 16 July 2007; Revised 1 April 2008; Accepted 30 April 2008*

## 1. Introduction

Climate, one of the main elements of the natural environment, has a determining role in natural and human life. Temperature, being one of the most important climatic parameters, has a direct impact on the evaporation, snow melting, frost and an indirect impact on the atmospheric stability and precipitation conditions (Erinc, 1957).

According to the recent climate change impact assessment studies framework, agriculture, vegetation, water resources and tourism are the sectors affected directly by temperature changes. Therefore, there is a need to forecast temperature accurately in order to prevent unexpected hazards caused by temperature variation, such as frost and drought which may cause financial and human losses (Kaymaz, 2005).

The study areas, Geyve and Sakarya, are located in the south-east of the Marmara region where a significant fraction of Turkey's agricultural production takes place. The Marmara and the Black Sea climate types are observed in this region (Unal *et al.*, 2003; Ikiel, 2005).

Climatic conditions have a crucial effect on the variability and production of crops while the economy of

the region is based on agriculture. The most important crops for this region are cherry, quince, peach, pear, grape, olive, corn and nut. Fruits are particularly sensitive to extreme temperature values and in certain years, temperature variations have a direct impact on the crop production and productivity. For example, Geyve is the nation's top quince producing area, but the frost on 8 April 2004 in Geyve decreased the productivity by 93% dropping the production from 17 885 to 1277 t (Kaymaz and Ikiel, 2004). After this year, in 2005, production of quince increased to 44 190 t (TMARA, 2005). In the future, according to the Intergovernmental Panel on Climate Change (IPCC) report's predictions, the temperature of the world will increase on average 1.8–6.4 °C (IPCC, 2007). The reflections of these predictions on Turkey can be disastrous. The yield in the agriculture sector will probably be lower causing an increase on the prices of the fresh fruits and the vegetables. In 2006, Turkey suffered a lot from drought especially in the agricultural sector. Because of these reasons, temperature forecasting is quite significant for agricultural activities.

In climate studies, numerical and statistical methods are used as forecasting methods. Numerical methods are used to simulate the atmospheric evolution in order to define the current weather changes. They use the global scale model outputs by converting them to daily

\* Correspondence to: B. Ustaoglu, Istanbul Technical University, Eurasia Institute of Earth Sciences, 34469 Maslak, Istanbul, Turkey.  
E-mail: beyza.ustaoglu@itu.edu.tr

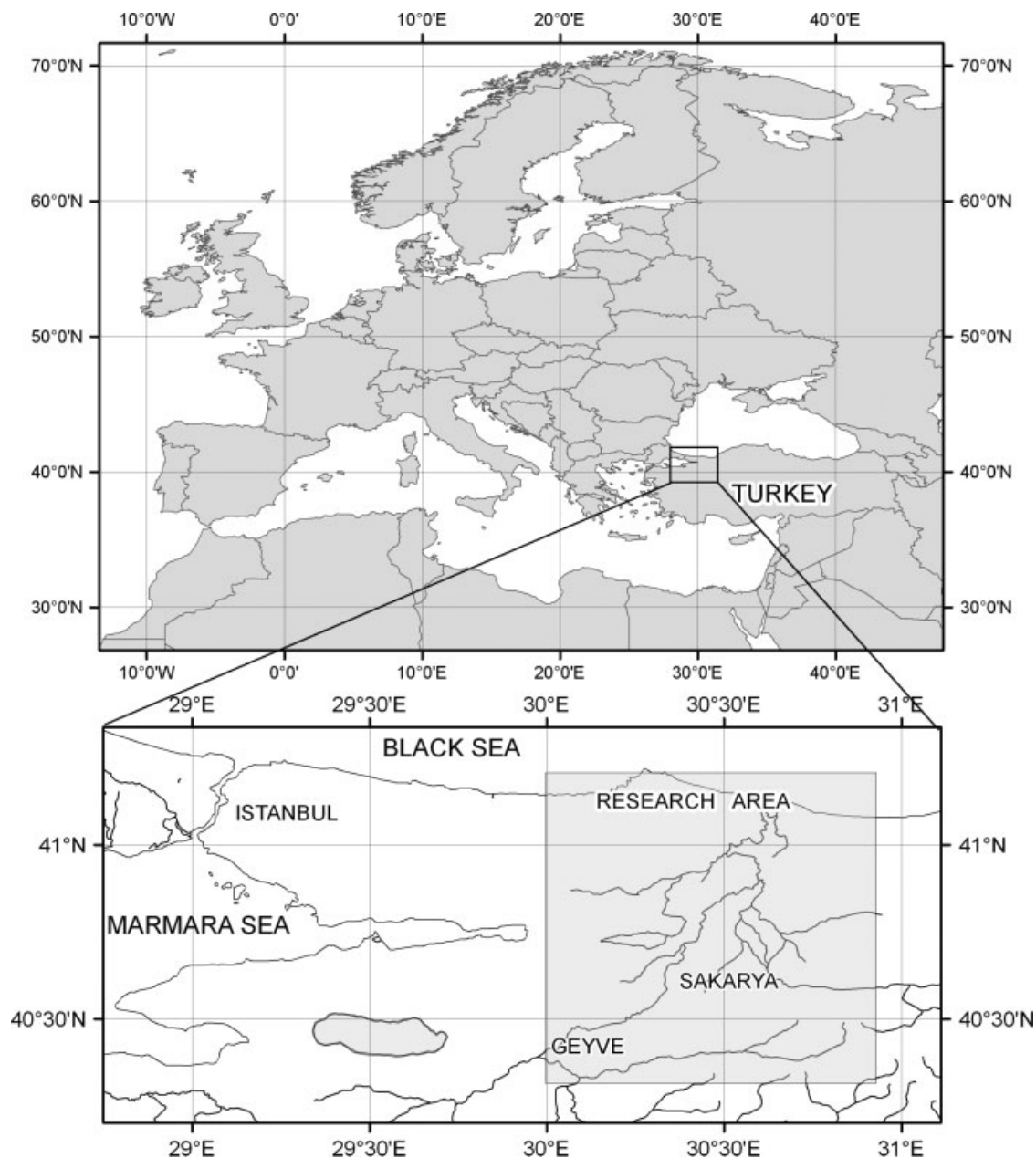


Figure 1. Location map of the research area (Geyve and Sakarya).

weather variables. Accordingly the downscaling technique is employed to convert the global scale model outputs to the regional or local scale (Kindap *et al.*, 2006). The applications of these methods provide particularly long-term period predictions and also give the best results on the large and regional scales for present and future climate events. On the other hand, statistical methods are based on observed relationships between the predictands and the predictors and they can be combined with numerical methods. They play key roles in the forecasting of the weather and the climate on time scales ranging from hours to several seasons. They have been applied to large, regional and local scale areas and determine the potential predictability of the climate and the weather to develop schemes for initializing the dynamical models,

for post-processing dynamical forecasts and to forecast the future weather and climate empirically (Zwiers and Storch, 2004). These methods are, respectively; (1) linear regression and correlation analysis, (2) principal component analysis, and, (3) canonical correlation analysis and singular value decomposition.

The artificial neural network (ANN) approach, which is a black box method, has been applied because of its high potential for complex, non-linear and time-varying input–output mapping (Dibike and Coulibaly, 2006). It has been frequently used in the northern hemisphere countries for the forecasting, recognition and classification purposes of many weather events (ASCE, 2000). The unique structure of the network and the non-linear transfer function combined with each hidden and output node

Table I. Statistical parameters (mean  $\bar{x}$ , maximum  $x_{\max}$ , minimum  $x_{\min}$  temperature, standard deviation  $\sigma$ , skewness  $c_{sx}$ , variance  $\sigma^2$ ) of Geyve and Sakarya daily temperature time series.

Daily temperature (°C)		$\bar{x}$			$x_{\max}$			$x_{\min}$		
Time series		Whole data	Training	Testing	Whole data	Training	Testing	Whole data	Training	Testing
Statistical parameters		01.01.1989	01.01.1989	26.12.2000	01.01.1989	01.01.1989	26.12.2000	01.01.1989	01.01.1989	26.12.2000
		31.12.2003	25.12.2000	31.12.2003	31.12.2003	25.12.2000	31.12.2003	31.12.2003	25.12.2000	31.12.2003
Geyve	$\bar{x}$	13.7	13.6	14.0	18.3	18.2	18.7	9.8	9.7	10.1
	$x_{\max}$	30.8	30.6	30.8	41.3	41.3	39.5	25.9	25.6	25.9
	$x_{\min}$	−7.8	−7.8	−5.2	−3.5	−2.8	−3.5	−13.1	−13.1	−12.0
	$\sigma$	7.8	7.8	8.0	9.0	9.0	9.1	7.6	7.6	7.8
	$\sigma^2$	61.2	60.7	63.5	81.9	81.2	84.5	58.4	58.0	60.2
	$c_{sx}$	−0.1	−0.1	−0.1	−0.1	−0.1	−0.1	−0.1	−0.1	−0.1
Sakarya	$\bar{x}$	14.4	14.3	15.0	18.8	18.6	19.5	11.2	11.1	11.7
	$x_{\max}$	31.6	31.6	30.1	42.7	42.7	38.7	27.2	25.9	27.2
	$x_{\min}$	−3.5	−3.5	−2.0	−2.4	−2.4	−0.7	−7.6	−7.6	−7.4
	$\sigma$	7.4	7.3	7.6	8.9	8.8	9.1	7.0	7.0	7.1
	$\sigma^2$	54.7	53.9	57.2	78.7	77.7	82.4	48.9	48.3	50.7
	$c_{sx}$	−0.2	−0.2	−0.2	−0.2	−0.2	−0.2	−0.1	−0.1	−0.1

allows ANNs to approximate highly non-linear relationships without *a priori* assumption. Furthermore, while other regression techniques assume a functional form, ANNs allow the data to define the functional form. Therefore, ANNs are generally believed to be more powerful than the other regression-based techniques (Cigizoglu, 2003a; Dibike and Coulibaly, 2006).

In a recent survey, Maier and Dandy (2000) report many applications of neural networks in forecasting water resource variables but, especially, studies on the forecast of temperature statistics, such as mean, maximum and minimum temperature are quite limited. In Turkey, particularly, studies of temperature forecasts have been very limited. Although in recent years a number of papers within the climatology community have adopted ANNs, this is the first study in Turkey to forecast daily mean, maximum and minimum temperatures using ANN methods and compare them with multiple linear regression (MLR).

The ANN approach has been successfully employed in the atmospheric sciences (Gardner and Dorling, 1998). In particular, temperature forecasting has already been analysed in some papers (Jang and Viau, 2004; Smith *et al.*, 2005, 2006). A number of authors have adopted ANN as a tool to downscale from the large scale atmospheric circulation to local or regional climate variables (Hewitson and Crane, 1992; Cavazos, 1997). Some applications have been made to construct climate change scenarios (Hewitson and Crane, 1996; Crane and Hewitson, 1998; Trigo and Palutikof, 1999).

ANN models have been used to forecast problems at an annual and seasonal scale (Tang *et al.*, 1994; Tangang *et al.*, 1998; Ramirez *et al.*, 2005) and short-term (hourly, monthly) predictions (Kuligowski and Barros, 1998; Cigizoglu, 2003a, 2004, 2005a,b; Jang and Viau, 2004; Freiwan and Cigizoglu, 2005; Cigizoglu and Alp, 2006; Cigizoglu and Kisi, 2006; Smith *et al.*, 2006). On the

other hand, in most of the studies the results obtained from complex ANN models were compared with those from more standard linear techniques such as regression (Schoof and Pryor, 2001; Bryant and Shreeve, 2002; Alp and Cigizoglu, 2007; Zhigang *et al.*, 2005). Also, the ANNs and stochastic methods (autoregressive (AR) and autoregressive moving average (ARMA)) were compared in some studies (Elsner and Tsonis, 1992; Mihalakakou *et al.*, 1998; Cigizoglu, 2003b).

The purpose of the present paper is the employment of three different ANN methods, feed-forward back propagation (FFBP), radial basis function (RBF) and generalized regression neural network (GRNN) to forecast temperature statistics such as daily mean temperature, daily maximum temperature and daily minimum temperature and to provide a best-fit prediction with the observed data using ANN algorithms. Additionally, predictions with a multiple linear regression (MLR) model were compared with those of the ANN methods. The methods were applied to temperature data from the Geyve and Sakarya meteorological stations.

## 2. Data description

Daily mean, maximum and minimum temperature time series data from the Geyve and Sakarya meteorological stations were used. These stations are located in the south-east of Marmara region in north-west Turkey 40°31.2'N, 30°16.8'E (Geyve) and 40°46.2'N, 30°22.8'E (Sakarya) with elevations of 30 and 100 m, respectively, above sea level (Figure 1). The data period spans from 1989 to 2003. The important statistical properties of the temperature time series are given in Table I and the whole seasonal record is plotted in Figure 2. The entire record (5468 days) was divided into two parts as training (80%) and testing (20%) periods.

Accordingly, the first 4374 daily mean temperature values constitute the training period, whereas the last 1094 daily mean temperature values were employed for the testing purpose. The daily statistical parameters, i.e. mean, maximum and minimum temperatures, standard deviation, skewness and variance of the data are computed and shown in Table I.

The statistics given in Table I show the differences between the stations. The daily mean, maximum and minimum temperature statistics of Geyve (G) are lower than those of Sakarya (S) [mean: 13.7 °C (G); 14.5 °C (S); maximum: 30.8 °C (G); 31.6 °C (S); minimum: −7.8 °C (G); −3.5 °C (S)]. The skewness values show that the temperature time series are nearly normally distributed (Table I). The ratio of standard deviation to mean value, the coefficient of variation ( $c_v$ ), is computed on the yearly basis and for each month separately for the daily mean temperature series of two stations (Table II). The autocorrelation coefficients of the daily temperature mean, maximum and minimum series for both stations are presented in Table III. It is clear that the daily temperature time series have relatively high auto-correlation coefficients in both locations. For the data series, the auto-correlation values are close to each other. The correlogram show that the correlation values do not decrease noticeably until lag 7 for both stations (Table III).

The cross-correlations between the Geyve and Sakarya daily temperature time series are presented in Table IV. Here  $r_{S,G,0}$  represents the correlation between the Geyve measurement at day 't' and the Sakarya measurement at day 't'. The  $r_{S,G,1}$  parameter corresponds to the correlation between the Geyve measurement at day 't' and the Sakarya measurement at day 't − 1'. Accordingly, the highest cross-correlation coefficients are found in the daily temperature time series between the Geyve and Sakarya both at day 't' ( $r_{S,G,0}$ ). As can be seen, the following cross-correlation coefficients for the next lags [time t (Geyve) and time t − i (Sakarya)] are also quite high.

When the maximum, minimum and mean temperature time series of both stations are plotted on a seasonal basis both data sets are hard to distinguish (Figure 2). The temperatures observed in both stations for the period 1989–2003 are close to each other. This is mainly because the topography, the morphology and the atmospheric conditions of the regions of two stations are similar to each other (Kaymaz and Ikiel, 2004). Slight differences in the temperature are significant when the temperature data are evaluated statistically. For example, 0.5 °C increase in the global mean temperature can affect water resources, agriculture and stock-breeding.

Table II. Coefficient of variation,  $c_v$  (%), of Geyve and Sakarya daily mean temperature time series (°C).

Month/ $c_v$ (%)	I	II	III	IV	V	VI	VII	VIII	IX	X	XI	XII	Annual
Geyve	62.7	42.8	28.4	15.6	6.7	2.9	4.9	4.5	7.5	8.8	13.2	30.4	4.9
Sakarya	34.4	32.9	27.9	16.5	7.0	3.0	5.5	4.8	7.6	8.7	13.9	25.7	4.8

Table III. Auto-correlation coefficients ( $r_1, r_2, \dots, r_7$ )<sup>a</sup> of Geyve and Sakarya daily temperature time series.

1989–2003	Data	$r_1$	$r_2$	$r_3$	$r_4$	$r_5$	$r_6$	$r_7$
Geyve	$\bar{x}$	0.96	0.92	0.89	0.87	0.86	0.85	0.84
	$x_{\max}$	0.91	0.85	0.81	0.78	0.77	0.76	0.75
	$x_{\min}$	0.94	0.89	0.87	0.86	0.84	0.84	0.84
	$\bar{x}$	0.95	0.89	0.85	0.83	0.81	0.80	0.79
Sakarya	$x_{\max}$	0.90	0.82	0.78	0.75	0.73	0.72	0.72
	$x_{\min}$	0.93	0.87	0.84	0.82	0.80	0.79	0.79

<sup>a</sup>  $r_1$  represents the lag 1 auto-correlation value, i.e. the correlation between the temperature measurement at day 't' and the temperature measurement at day 't − 1'. Similarly  $r_2$  corresponds to the correlation between the measurements at days 't' and 't − 2'.

Table IV. Cross-correlations ( $r_{S,G,0}, r_{S,G,1}, \dots, r_{S,G,7}$ )<sup>a</sup> between Geyve (G) and Sakarya (S) daily temperature time series.

Sakarya/Geyve	$\bar{x}$ °C	$x_{\max}$ °C	$x_{\min}$ °C
$r_{S,G,0}$	0.98	0.99	0.96
$r_{S,G,1}$	0.95	0.91	0.93
$r_{S,G,2}$	0.91	0.84	0.89
$r_{S,G,3}$	0.87	0.79	0.86
$r_{S,G,4}$	0.85	0.77	0.84
$r_{S,G,5}$	0.83	0.75	0.83
$r_{S,G,6}$	0.82	0.74	0.82
$r_{S,G,7}$	0.82	0.73	0.81

<sup>a</sup>  $r_{S,G,0}$  represents the correlation between the Geyve temperature measurement at day 't' and the Sakarya temperature measurement at day 't'. The  $r_{S,G,1}$  parameter corresponds to the correlation between the Geyve measurement at day 't' and the Sakarya measurement at day 't − 1'.

A cyclical behaviour is observed for each year (Figure 2). This is mainly because the seasonal and yearly variations in the temperature series are quite low when compared to other meteorological series such as rainfall and wind. Only the coefficient of variation values for the winter months December, January and February within the period 1989–2003 are high (Table II). This is related to the intense transfer of the various air masses and the movement of cyclones during the winter months. On the annual basis, however, the coefficient of variation values are quite low, i.e. 4.9 and 4.8% for Geyve and Sakarya respectively (Table II).

### 3. Artificial neural network (ANN)

The ANN is a system predicting human brain learning and thinking behaviour using measured or observed

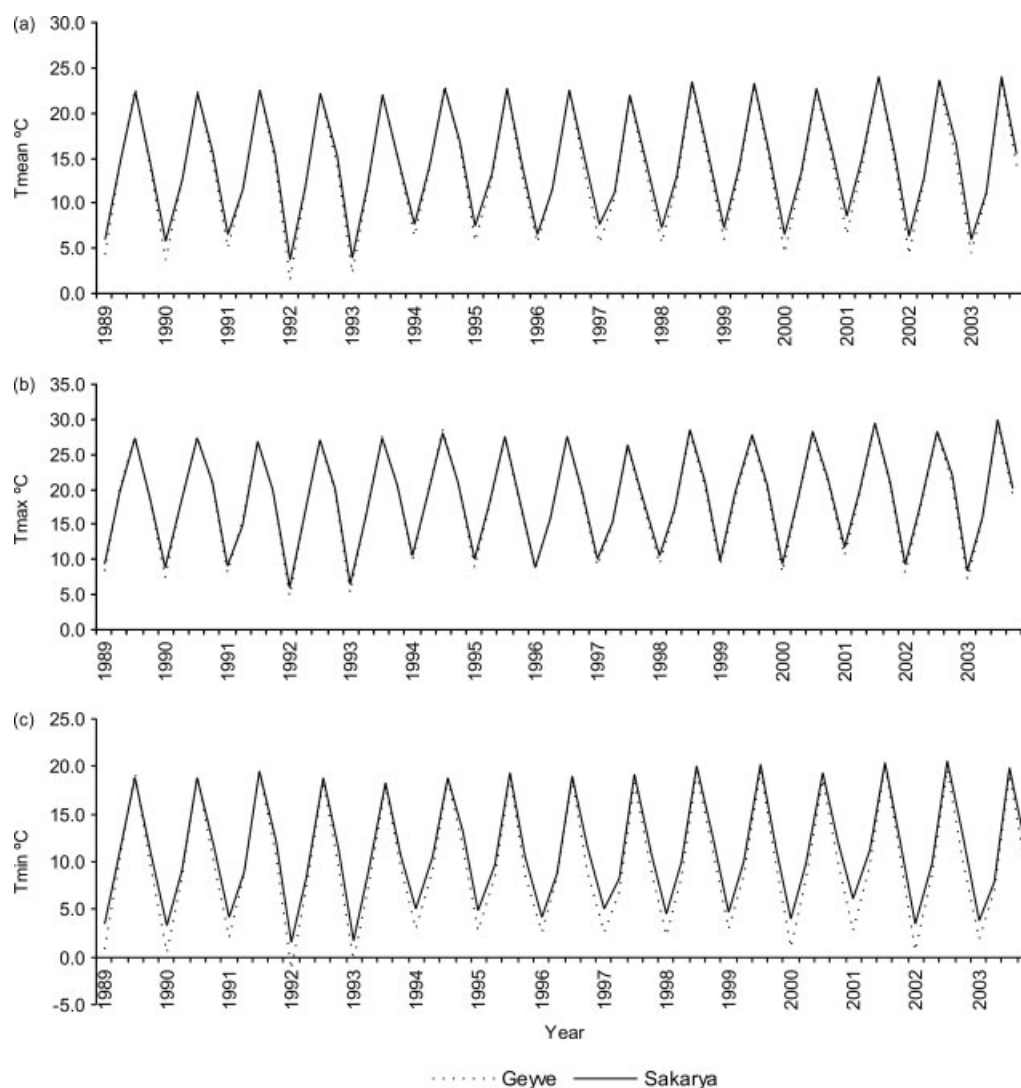


Figure 2. The seasonal mean (a), maximum (b) and minimum (c) temperature time series for the period of 1989–2003 in Geyve (· · · · ·) and Sakarya (—).

data. It is widely used to solve problems too difficult to solve by conventional mathematical methods. They are computer-based problem solving tools inspired by the original, biological neural network – the brain. Because of their ability to generate non-linear mappings during training, ANNs are particularly well suited to complex, real-world problems such as understanding climate (Elsner and Tsonis, 1992). A focus of the study is to assess the efficiency of the ANNs in forecasting the daily mean, maximum and minimum temperature. Three MATLAB codes were written for the three types of ANN, first, for the FFBP Algorithm, second, for the RBF algorithm and the last one for the GRNN. For the FFBP, the Levenberg–Marquardt technique was preferred because of its rapid convergence advantage (Cigizoglu and Alp, 2006).

### 3.1. Feed-forward back propagation (FFBP)

All ANN modules are based on the FFBP model. Given a training set of input–output data, the most common

learning rule for multilayer perceptions is the back-propagation algorithm (BPA). Back propagation involves two phases: a feed-forward phase in which the external input information at the input nodes is propagated forward to compute the output information signal at the output unit, and a backward phase in which modifications to the connection strengths are made based on the differences between the computed and observed information signals at the output units (Alp and Cigizoglu, 2007). The neural network structure in this study possessed a three-layer learning network consisting of an input layer, a hidden layer and an output layer (Figure 3). The FFBP configuration consists of an input layer, one or more hidden layers and an output layer. In a feed-forward network, the input quantities are fed to the input nodes, which in turn pass them on to the hidden layer nodes after multiplying by a weight. A hidden layer node, the function of which is to intervene between the external input and the network output, adds up the weighted input received from each input node, associates it with a bias, and then passes the result on to the nodes of the next hidden layer or the

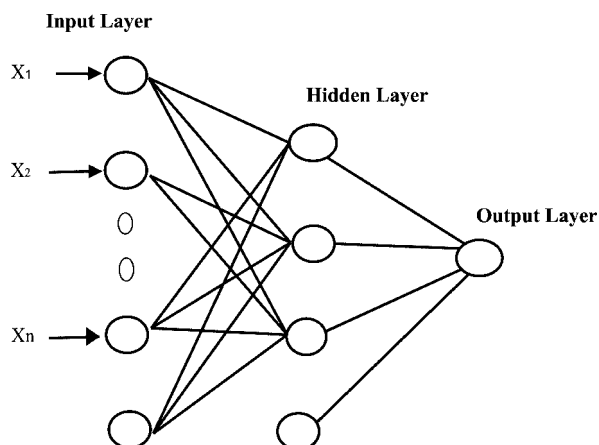


Figure 3. The structure of the feed-forward back-propagation neural network (FFBP).

output, through a non-linear transfer function. The learning process works in small iterative steps. The output is compared to the known-good output, and a mean square error signal is calculated. The error value is then propagated backwards through the network, and small changes are made to the weights in each layer. The weight changes are calculated to reduce the error signal for the case in question. The cycle is repeated until the overall error value drops below some predetermined threshold. The FFBP was trained using the Levenberg–Marquardt optimization technique. This optimization technique is more powerful than the conventionally used gradient descent techniques (Cigizoglu and Kisi, 2006). Throughout all FFBP simulations, the learning rate and the momentum rate, parameters which accelerate the FFBP simulation duration, were taken adaptively. The learning rate and the momentum rate are decreased if the difference between consecutive mean square error values start to decrease and increased if it was the opposite case. Several iteration numbers between 50 and 1500 were tested for the training period of FFBP. For each iteration number option the trained neural network was employed for the test data. The iteration number 100 provided the lowest mean square error (MSE) and highest  $R^2$  for the testing period data. This procedure was explained and employed in previous neural network studies of water resources (Cigizoglu, 2003a, 2004).

### 3.2. Radial basis function (RBF)

RBF networks were introduced into the neural network literature by Broomhead and Lowe (1988). The RBF network is a feed-forward type of ANN. The RBFs are one of the most famous training algorithms for multilayer perceptions (Figure 4). These groups of neural network employ units with localized receptive fields, where units receiving direct input from input signals (patterns) can only see a part of the input pattern. The pattern of connectivity and the number of neurons in each layer may vary within some constraints. No communication is permitted between the nodes within a layer, but the nodes

in each layer may send their output to the nodes in the succeeding layers. The nodes receive input either from the initial inputs or from the interconnections. Different numbers of hidden layer neurons and spread constants are examined in the study. The number of neurons in the hidden layer that give the minimum MSE were found to vary between 5 and 13. This spread is a constant which is selected before RBF simulation. The spreads that give the minimum MSE are between 0.03 and 6.3. These were found with a simple trial-error method adding some loops to the programme codes.

### 3.3. Generalized regression neural network (GRNN)

General regression neural networks are a variant of radial basis ANNs and are often used for function approximation (Specht, 1991). It approximates any arbitrary function between input and output vectors, drawing the function estimate directly from the training data (Figure 5). In addition, it is consistent that as the training set size becomes large, the estimation error approaches zero, with only mild restrictions on the function. The GRNN is used for the estimation of continuous variables, as in standard regression techniques. It is related to the RBF network and is based on a standard statistical technique called kernel regression. The principal advantages of the GRNN are fast learning and convergence to the optimal regression surface as the number of samples becomes very large. It is particularly advantageous with sparse data in a real-time environment, because the regression surface is instantly defined everywhere, even with just one sample (Cigizoglu, 2005). The success of the GRNN method depends heavily on the spread factors (Specht, 1991) the larger the spread, the smoother the function approximation. Too large a spread means a lot of neurons will be required to fit a fast changing function. Too small a spread means many neurons will be required to fit a smooth function, and the network may not generalize well. The spread values between 0 and 1 were employed to obtain the minimum MSE for the testing period.

### 3.4. Comparison of the ANN methods

In the majority of ANN studies in hydrometeorology the FFBP method has been employed to train the neural networks. The performance of FFBP was found superior to conventional statistical and stochastic methods in continuous flow series forecasting (Brikundavyi *et al.*, 2002; Cigizoglu, 2003a,b). However, the FFBP algorithm has some drawbacks. It is very sensitive to the selected initial weight values and may provide performances significantly differing from each other. Another problem faced during the application of FFBP is the local minima issue. During the training stage, the networks are sometimes trapped by the local error minima preventing them reaching the global minimum. Maier and Dandy (2000) summarized the methods used in the literature to overcome

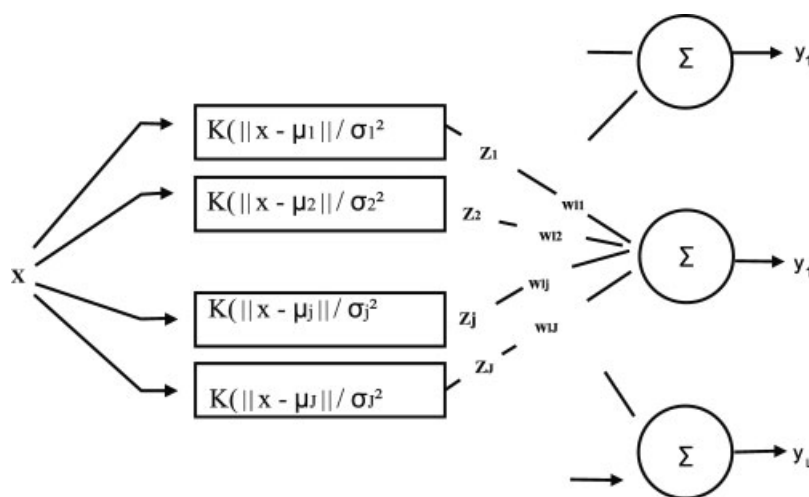


Figure 4. The structure of the radial basis function neural network (RBF).

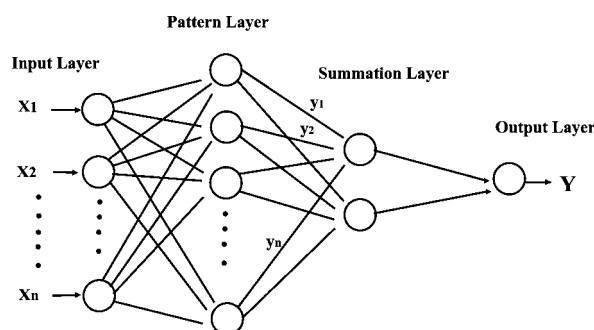


Figure 5. The structure of the generalized regression neural network (GRNN).

the local minima problem, by training a number of networks starting with different initial weights, the on-line training mode to help the network to escape local minima, inclusion of the addition of random noise, employment of second order (Newton algorithm, Levenberg–Marquardt algorithm) or global methods (stochastic gradient algorithms, simulated annealing). In the review study of the ASCE Task Committee (2000) other ANN methods, such as conjugate gradient algorithms, RBF, cascade correlation algorithm and recurrent neural networks, were briefly explained. Thirumalaiah and Deo (1998, 2000) used conjugate gradient and cascade correlation algorithms together with FFBP for different hydrological applications. Levenberg–Marquardt algorithm was employed in the FFBP applications included in the presented study.

Because of these drawbacks with the FFBP algorithm it is necessary to investigate other ANN algorithms. The performance of one of such alternate ANN, the GRNN algorithm, was found to be superior to the FFBP in intermittent daily river flow forecasting (Cigizoglu, 2005b). The simulation studies with FFBP showed that different forecasting performances were obtained after each simulation with the same network structure. This is mainly due to the assignment of different initial random weights in the beginning of each training simulation. Each time, the FFBP network was trapped by the different

local error minima and thus global minimum was not attained. This issue was examined in detail by Cigizoglu (2004).

The forecast of the GRNN is bounded by the minimum and maximum of the observed series, preventing network-providing forecasts which are not physically possible. The GRNN and RBF networks learn in one pass through the data and can generalize from examples as soon as they are stored (Specht, 1991). The FFBP training, however, requires much iteration to converge. The GRNN forecasts cannot converge to poor solutions corresponding to local minima of the error criterion, which is one of the drawbacks of the FFBP algorithm.

The only disadvantage of the GRNN is its longer training duration compared to FFBP. However, it was seen that many FFBP simulations are required in order to select the one with satisfactory performance criteria. The FFBP simulations are sensitive to the randomly assigned initial values of correlation weights. This total duration of the FFBP simulations is longer than the unique GRNN application. On the other hand, the GRNN algorithm, which uses clustering (Specht, 1991), overcomes this problem but this algorithm was not employed in this study.

#### 4. Multiple linear regression (MLR)

MLR is the least computationally demanding downscaling technique and has been widely used in atmospheric science (Schoof and Pryor, 2001) in time series analyses. It is usually less complicated than its non-linear counterparts with lower demands regarding computational power, and, unlike non-linear methods, without many parameters to be determined prior to their application. It attempts to model the relationship between two or more explanatory variables and a response variable by fitting a linear equation to observed data. Every value of the independent variable  $x$  is associated with a value of the dependent variable  $y$ . The general equation is as follows:



If  $y$  is a dependent variable and  $x_1, x_2, \dots, x_i$  are independent variables, then the basic model is given in Equation (1);

$$y = a + b_1 + x_1 + b_2x_2 + \dots + b_ix_i + e \quad (1)$$

where  $a, b_i$  = constant and  $e$  = random variable (Holder, 1985).

## 5. Method

The ANN methods, FFBP, RBF, GRNN and the MLR method, have been applied to the time series of daily mean temperature ( $T_{\text{mean}}$ ), daily maximum temperature ( $T_{\text{max}}$ ) and daily minimum temperature ( $T_{\text{min}}$ ).

Using two meteorological stations (Geyve and Sakarya), three different cases were considered in the presented study of which the first two cases, the temperature time series of each station was forecasted using the past daily measurements.

In the third case, the temperature time series of a station (Geyve) was forecasted using the data of the neighbouring station (Sakarya). This was noted for example as  $T_{\text{meanSG}}$  representing the forecasted Geyve data using the values of Sakarya as input. The application of the ANNs to the temperature time series data consisted of two steps. The first step is the training of the neural networks. It comprises the presentation of daily temperature data describing the input and output to the network and obtaining the inter connection weights. The input layer elements have been composed of the temperature values of previous days. For the number of the input values, different choices have been selected and their results examined. The time series have been modelled by using only the past seven daily values of the predictand (times  $t - 7, \dots, t - 1, t$ ) to forecast the value at time  $t$  for daily mean, maximum and minimum temperature time series. For each selected number of inputs, the correlation coefficient ( $R$ ), the root mean square error (RMSE) and index of agreement (IA) have been calculated and presented in Table V. Once the training stage was completed, the ANNs were applied to the testing data.

Determining an appropriate architecture of a neural network for a particular problem is an important issue, since the network topology directly affects its computational complexity and its generalization capability. The number of hidden layer spread parameters and the number of nodes in the input and hidden layers were determined after trying various networks. In fact, the effect of the number of nodes in the hidden layer on the forecasting performance is not as significant as the number of nodes in the input layer (Cigizoglu, 2004).

Before training and testing, the data are scaled using the extremes between 0 and 1 for each NN models as given in Equation (2):

$$x_i^{\text{scaled}} = \frac{x_i - x_{\text{min}}}{x_{\text{max}} - x_{\text{min}}} \quad (2)$$

where  $x_i, x_{\text{max}}$  and  $x_{\text{min}}$  are the original, the maximum and the minimum values respectively. A periodicity index was then used in the input layer. The periodicity index has the importance of showing the effects of the seasons on the forecasts of neural networks. It is computed by ratios between  $1/365$  and 1 for each of the 365 days of the year. The only parameter which should be adjusted in FFBP simulations is the hidden layer node number. In the RBF simulations, the spread parameter  $s$ , should be found and in the GRNN simulations, the smoothing parameter,  $\sigma$ , is adjusted (Cigizoglu, 2005a,b). For the purpose of comparison, MLR was also employed. Accordingly, the independent variables of MLR are the input nodes of the ANNs and the calibration period is the ANN training duration.

For the comparison using the FFBP, RBF, GRNN and MLR, the performance of methods have been evaluated in terms of the selected performance criteria:  $R$ , RMSE and IA. The IA is a dimensionless index bounded between 0 (showing no agreement at all) and 1 (perfect agreement of the time series) (Jorquera *et al.*, 1998).

The IA Equation (3) is as follows:

$$IA = 1 - \frac{\sum_{i=1}^N (x_i - y_i)^2}{\sum_{i=1}^N (|x'_i| + |y'_i|)^2} \quad (3)$$

where  $x$  is the mean value of the observed, and  $y$  is the mean value of the forecasted,  $x_i$  is the value observed at the  $i$ th time step,  $y_i$  is the value forecasted at the same moment of time,  $N$  is the number of time steps,  $y'_i = (y_i - x_m)$  and  $x'_i = (x_i - x_m)$  (Makarynskyy *et al.*, 2004).  $R$  provides the variability measure of the data reproduced in the model. RMSE measures residual errors which give a global idea of the difference between the observed and modelled values (Gardner and Dorling, 2000).

## 6. Forecasting results

In this part of the study, one-day-ahead forecasting has been carried out using precedent daily mean, maximum and minimum temperature time series using FFBP, GRNN, RBF and MLR. Originally the forecasting of the daily temperature values using the past seven daily observations at the same station were included, then this was extended by incorporating the data of the neighbouring station to the input layer. Accordingly the data of the Sakarya station were also considered in the forecasting of the Geyve data. For each temperature forecasting case,  $R$ , RMSE and IA were calculated and presented in Table V and Figure 6.

### 6.1. Forecasting daily mean temperature ( $T_{\text{mean}}$ )

The FFBP, GRNN, RBF and MLR methods have been employed to forecast the daily mean temperature time

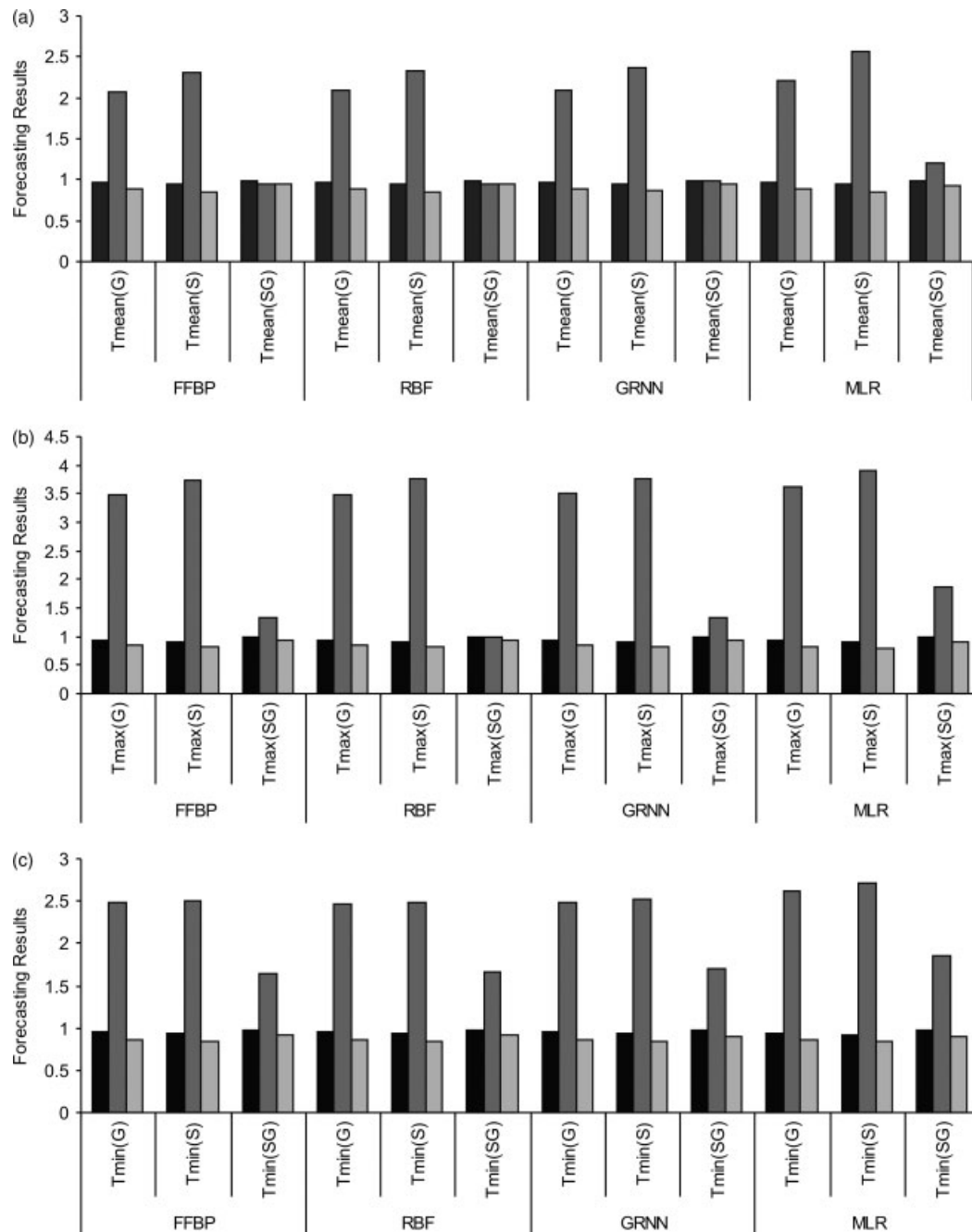


Figure 6. The mean (a), maximum (b) and minimum (c) temperature forecasting results for using different methods [feed-forward back propagation (FFBP), radial basis function (RBF), generalized regression neural network (GRNN), multiple linear regression (MLR)] and performance criteria [the correlation coefficient ( $R$  ■), the root mean square error (RMSE ■) and the index of agreement (IA ■)] for the testing period.

series. The most suitable ANN configuration for each method is given in Table V. In Geyve ( $T_{meanG}$ ), the highest  $R$  (0.970) was obtained by RBF, the lowest  $RMSE$  (2.08) by FFBP and the highest  $IA$  (0.896) by FFBP for the testing period. In Sakarya ( $T_{meanS}$ ), the highest  $R$  (0.955) was obtained by RBF, the lowest  $RMSE$  (2.31) by FFBP, and the highest  $IA$  (0.863) by GRNN and RBF for the testing period. In the neighbouring station ( $T_{meanSG}$ ), the highest  $R$  (0.993) was obtained by RBF, the lowest  $RMSE$  (0.94) by FFBP, and the highest  $IA$  (0.953) by FFBP for the testing period (Table V, Figure 6(a)). Prediction of the  $T_{mean}$  values for Geyve using the  $T_{mean}$  values of Sakarya and the past  $T_{mean}$  values of

Geyve provided superior performance criteria compared with the case where only the past Geyve  $T_{mean}$  was employed. Among the three cases  $T_{meanSG}$  provided the best forecasts according to the performance criteria;  $R = 0.993$  by RBF;  $RMSE = 0.94$  and  $IA = 0.953$  by FFBP (Table V, Figure 6(a)). While the RBF method gave the highest  $R$ , the FFBP method provided the lowest  $RMSE$  and highest  $IA$  values for  $T_{meanG}$  and  $T_{meanS}$ . Although both ANN and MLR techniques forecasted temperature relatively well for  $T_{meanG}$ ,  $T_{meanS}$ ,  $T_{meanSG}$ , the ANN outperformed MLR for the performance criteria, i.e.  $R$ ,  $RMSE$  and  $IA$ . While the FFBP performances gave reasonable performance providing close estimates

Table V. Forecasting results for using different methods and performance criteria<sup>a</sup> for the testing period.

Methods	Location	Temperature data	ANN structure <sup>b</sup>	<i>R</i>	<i>RMSE</i> (°C/day)	<i>IA</i>
FFBP	Geyve	$T_{\text{mean}}$	7,5,1	0.965	2.080	0.896
		$T_{\text{max}}$	7,5,1	0.925	3.490	0.839
		$T_{\text{min}}$	7,5,1	0.948	2.480	0.865
	Sakarya	$T_{\text{mean}}$	7,5,1	0.952	2.310	0.857
		$T_{\text{max}}$	7,5,1	0.911	3.750	0.821
		$T_{\text{min}}$	7,5,1	0.937	2.510	0.845
	Sakarya and Geyve	$T_{\text{mean}}$	7,5,1	0.992	0.940	0.953
		$T_{\text{max}}$	7,5,1	0.992	1.340	0.935
		$T_{\text{min}}$	7,5,1	0.981	1.640	0.916
	Geyve	$T_{\text{mean}}$	7,0.99,1	0.970	2.090	0.895
		$T_{\text{max}}$	7,0.55,1	0.927	3.490	0.839
		$T_{\text{min}}$	7,0.99,1	0.950	2.470	0.868
RBF	Sakarya	$T_{\text{mean}}$	7,0.99,1	0.955	2.330	0.857
		$T_{\text{max}}$	7,0.55,1	0.910	3.760	0.810
		$T_{\text{min}}$	7,0.99,1	0.942	2.480	0.845
	Sakarya and Geyve	$T_{\text{mean}}$	7,0.99,1	0.993	0.950	0.951
		$T_{\text{max}}$	7,0.55,1	0.993	1.000	0.942
		$T_{\text{min}}$	7,0.99,1	0.982	1.660	0.915
	Geyve	$T_{\text{mean}}$	7,0.05,1	0.964	2.100	0.892
		$T_{\text{max}}$	7,0.08,1	0.924	3.510	0.838
		$T_{\text{min}}$	7,0.07,1	0.947	2.490	0.864
	Sakarya	$T_{\text{mean}}$	7,0.05,1	0.950	2.360	0.863
		$T_{\text{max}}$	7,0.08,1	0.910	3.760	0.817
		$T_{\text{min}}$	7,0.07,1	0.935	2.530	0.841
GRNN	Sakarya and Geyve	$T_{\text{mean}}$	7,0.05,1	0.992	0.990	0.949
		$T_{\text{max}}$	7,0.08,1	0.989	1.340	0.941
		$T_{\text{min}}$	7,0.07,1	0.975	1.710	0.900
	Geyve	$T_{\text{mean}}$	—	0.960	2.220	0.883
		$T_{\text{max}}$	—	0.925	3.620	0.828
		$T_{\text{min}}$	—	0.942	2.610	0.860
	Sakarya	$T_{\text{mean}}$	—	0.941	2.560	0.848
		$T_{\text{max}}$	—	0.904	3.910	0.805
		$T_{\text{min}}$	—	0.925	2.710	0.832
	Sakarya and Geyve	$T_{\text{mean}}$	—	0.989	1.200	0.929
		$T_{\text{max}}$	—	0.980	1.860	0.915
		$T_{\text{min}}$	—	0.971	1.860	0.889

<sup>a</sup> The correlation coefficient (*R*), the root mean square error (*RMSE*) and the index of agreement (*IA*).

<sup>b</sup> An ANN structure FFBP (7, 5, 1) consists of 7, 5 and 1 nodes in input, hidden and output layers, respectively for  $T_{\text{mean}}$ . RBF (7, 0.99, 1) has 7 and 1 nodes in input and output layers, respectively, and a spread parameter was chosen to be 0.99 for  $T_{\text{mean}}$ . Similarly GRNN (7, 0.05, 1) has 7 and 1 nodes in input and output layers, and a spread parameter was chosen to be 0.05 for  $T_{\text{mean}}$ .

compared with other ANN methods and MLR in  $T_{\text{mean}}$  forecasting in terms of the selected performance criteria, *RMSE* and *IA*; the RBF performance provided superior performance in terms of *R*.

## 6.2. Forecasting daily maximum temperature ( $T_{\text{max}}$ )

One-day-ahead forecasting was performed using the precedent daily maximum temperature time series for FFBP, GRNN, RBF and MLR. The most convenient ANN configuration for each method is given in Table V. In Geyve ( $T_{\text{maxG}}$ ), the highest *R* (0.927) was obtained by RBF whereas the lowest *RMSE* (3.49) and the highest *IA* (0.839) belonged to FFBP and RBF for the testing period (Table V, Figure 6(b)). In Sakarya ( $T_{\text{maxS}}$ ), the highest *R* (0.911), the lowest *RMSE* (3.75) and the

highest *IA* (0.821) were obtained by FFBP for the testing period. In the neighbouring station ( $T_{\text{maxSG}}$ ), the highest *R* (0.993), the lowest *RMSE* (1.00) and the highest *IA* (0.942) were obtained by RBF for the testing period. Prediction of the  $T_{\text{max}}$  values for Geyve using the  $T_{\text{max}}$  values of Sakarya and the past  $T_{\text{max}}$  values of Geyve provided superior performance criteria compared to the case where only the past Geyve  $T_{\text{max}}$  were employed. The more accurate predictions were obtained for  $T_{\text{maxSG}}$  with the performance criteria *R* = 0.993; *RMSE* = 1.00; *IA* = 0.942 for RBF (Table V, Figure 6(b)). While the FFBP and RBF methods provided the highest *R*, they also gave the lowest *RMSE* value and the highest *IA* value for  $T_{\text{maxG}}$ ,  $T_{\text{maxS}}$  and  $T_{\text{maxSG}}$ . Although both ANN and MLR techniques forecasted temperature reasonably well

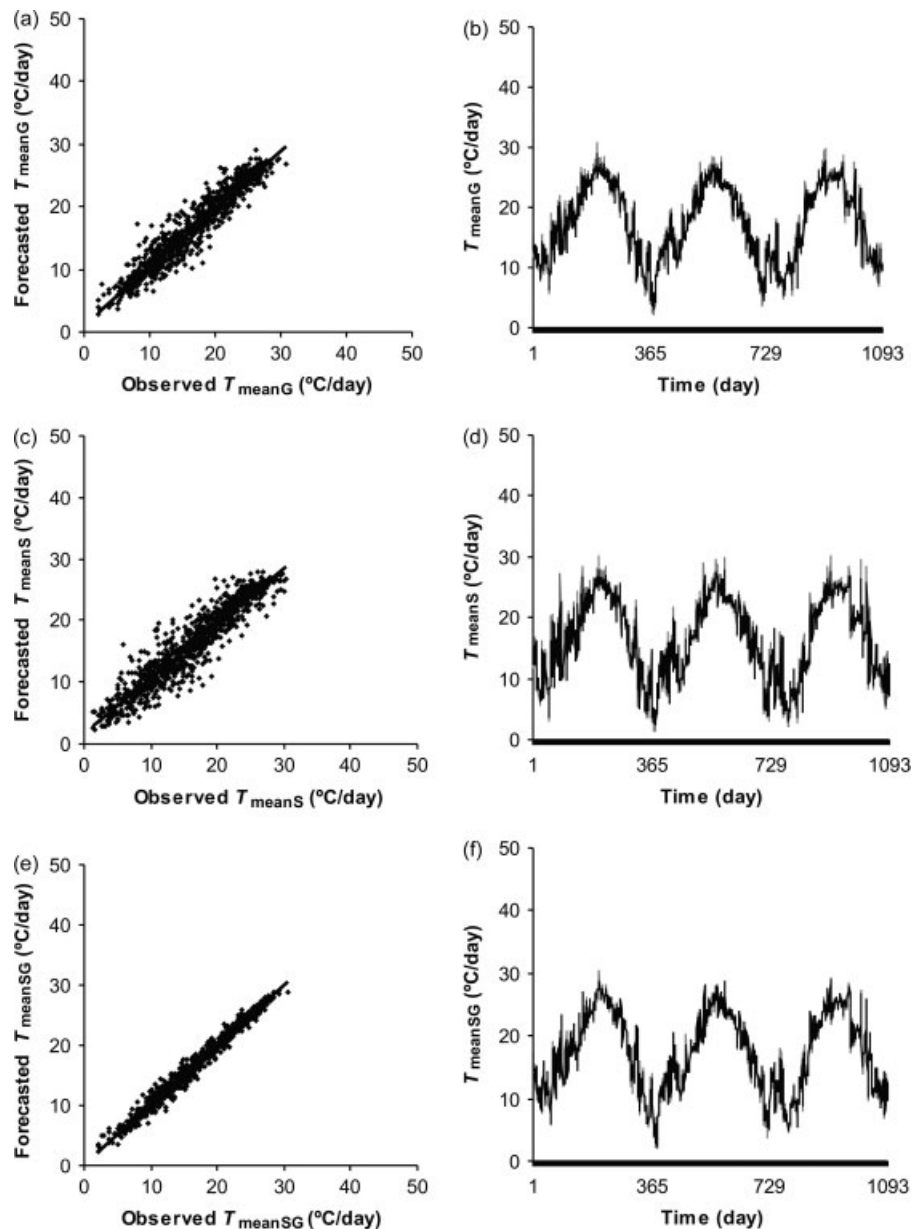


Figure 7. Forecasting daily mean temperature time series by RBF method in scatter graphic versus line graphic (a) and (b) for Geyve ( $T_{\text{meanG}}$ ), (c) and (d) for Sakarya ( $T_{\text{meanS}}$ ), (e) and (f) for neighbouring station ( $T_{\text{meanSG}}$ ).  $y$  is the equation used for forecast and  $R$  is the correlation coefficient between observed and forecasted values in graphics (a), (c) and (e). The grey line is the observed value; the black line is the forecasted value in graphics (b), (d) and (f). (a)  $y = 0.9257x + 1.6125$   $R^2 = 0.955$ ; (c)  $y = 0.8987x + 1.7945$   $R^2 = 0.955$ ; (e)  $y = 0.9879x + 0.3548$   $R^2 = 0.993$ .

for  $T_{\text{maxG}}$ ,  $T_{\text{maxS}}$ ,  $T_{\text{maxSG}}$ , the ANN outperformed MLR for the performance criteria, i.e.  $R$ , RMSE and IA. The FFBP and RBF methods performed satisfactorily providing close estimates compared with GRNN and MLR in  $T_{\text{max}}$  forecasting in terms of the selected performance criteria; RMSE,  $R$ , IA.

### 6.3. Forecasting daily minimum temperature ( $T_{\text{min}}$ )

In this part of the study, the FFBP, GRNN, RBF and MLR methods have been applied to the daily minimum temperature time series. The best-fit ANN configuration for each method is given in Table V. In Geyve ( $T_{\text{minG}}$ ), the highest  $R$  (0.950), the lowest RMSE (2.47) and the

highest IA (0.868) were obtained by RBF for the testing period. In Sakarya ( $T_{\text{minS}}$ ), the highest  $R$  (0.942) and the lowest RMSE (2.48) were obtained by RBF and the highest IA (0.845) by FFBP and RBF for the testing period. In the neighbouring station ( $T_{\text{minSG}}$ ), the lowest RMSE (1.64) was obtained by FFBP. On the other hand, the highest  $R$  (0.982) was presented by RBF and the highest IA (0.916) by FFBP (Table V, Figure 6(c)).

Forecasting the  $T_{\text{min}}$  values of Geyve using the  $T_{\text{min}}$  values of Sakarya and the past  $T_{\text{min}}$  values of Geyve provided superior performance criteria compared with the case where only the past Geyve  $T_{\text{min}}$  were employed. Among the stations the more accurate predictions were obtained for  $T_{\text{minSG}}$  ( $R = 0.982$  and  $IA = 0.916$  by RBF;

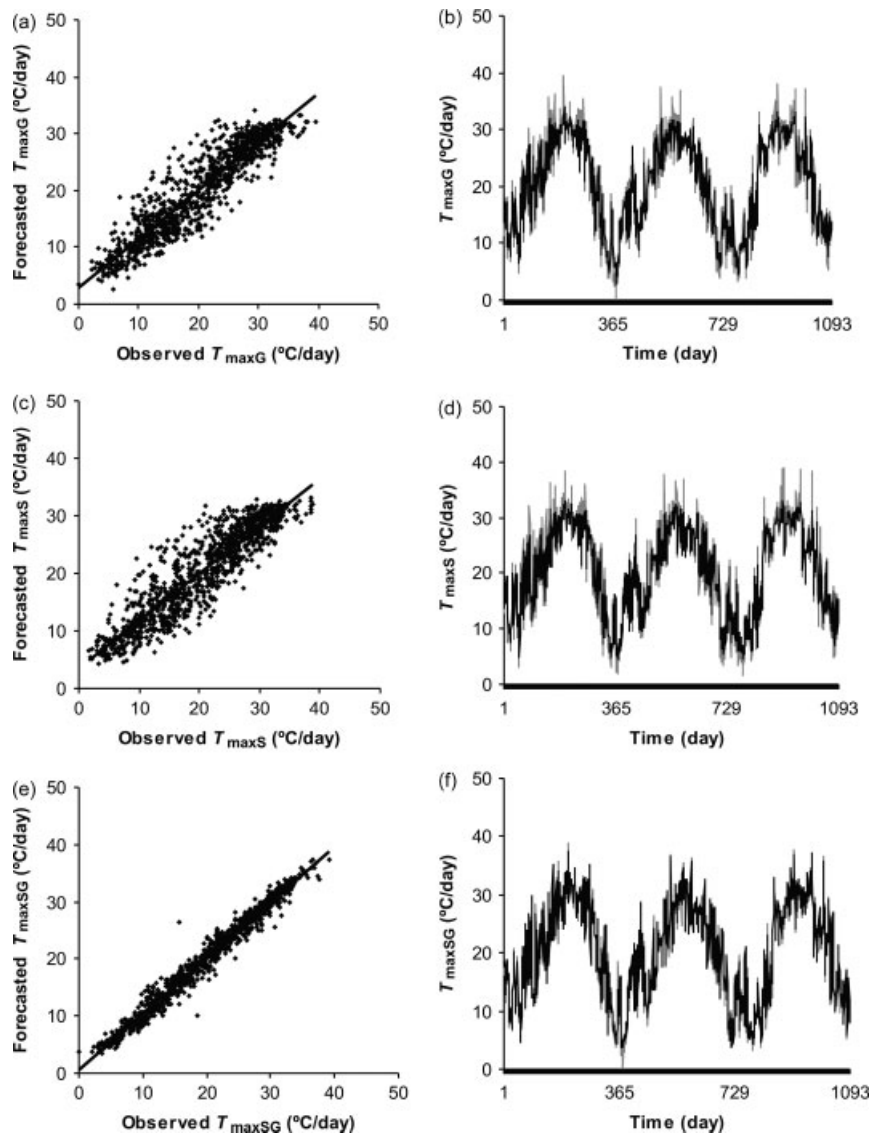


Figure 8. Forecasting daily maximum temperature time series by RBF method in scatter graphic *versus* line graphic (a) and (b) for Geyve ( $T_{\max G}$ ), (c) and (d) for Sakarya ( $T_{\max S}$ ), (e) and (f) for neighbouring station ( $T_{\max SG}$ ).  $y$  is the equation used for forecast and  $R$  is the correlation coefficient between observed and forecasted values in graphics (a), (c) and (e). The grey line is the observed value; the black line is the forecasted value in graphics (b), (d) and (f). (a)  $y = 0.8503x + 3.2671$   $R^2 = 0.927$ ; (c)  $y = 0.8166x + 3.8665$   $R^2 = 0.910$ ; (e)  $y = 0.9855x + 0.4878$   $R^2 = 0.993$ .

$RMSE = 1.64$  by FFBP; Table V, Figure 6(c)). While the RBF method had the highest  $R$ , the FFBP and RBF method provided the lowest  $RMSE$  value and the highest  $IA$  values for  $T_{\min G}$ ,  $T_{\min S}$  and  $T_{\min SG}$ . Although both ANN and MLR techniques forecasted temperature relatively well for  $T_{\min G}$ ,  $T_{\min S}$ ,  $T_{\min SG}$ , the ANN outperformed MLR for the performance criteria, i.e.  $R$ ,  $RMSE$  and  $IA$ . While FFBP and RBF performances were quite satisfactory providing close estimates compared with GRNN and MLR in forecasting  $T_{\min}$  in terms of the selected performance criteria,  $RMSE$  and  $IA$  the RBF performance provided superior performance in terms of  $R$ .

## 7. Discussion and conclusions

The objective of this study was to forecast the daily mean ( $T_{\text{mean}}$ ), maximum ( $T_{\text{max}}$ ) and minimum ( $T_{\text{min}}$ ) temperature time series using three different ANN methods and

provide the best-fit prediction with the observed actual data. Three different neural network methods, the FFBP, the RBF and the GRNN are employed using 15 years (1989–2003) for this purpose. Additionally, predictions with a MLR model were compared to those of the ANN methods. For the comparison using the FFBP, the RBF, the GRNN and the MLR methods, the performance of the methods has been evaluated in terms of the  $R$ ,  $RMSE$  and  $IA$  (Table V, Figure 6). The graphs of the best observed *versus* the forecasted values are plotted (Figures 7–9).

The results of the methods can be summarized as follows.

While the FFBP method performed quite well, compared with the other ANN methods and the MLR method, providing good agreement with the forecasts in daily mean temperature ( $T_{\text{mean}}$ ) forecasting in terms of the selected performance criteria,  $RMSE$  and  $IA$ , the RBF

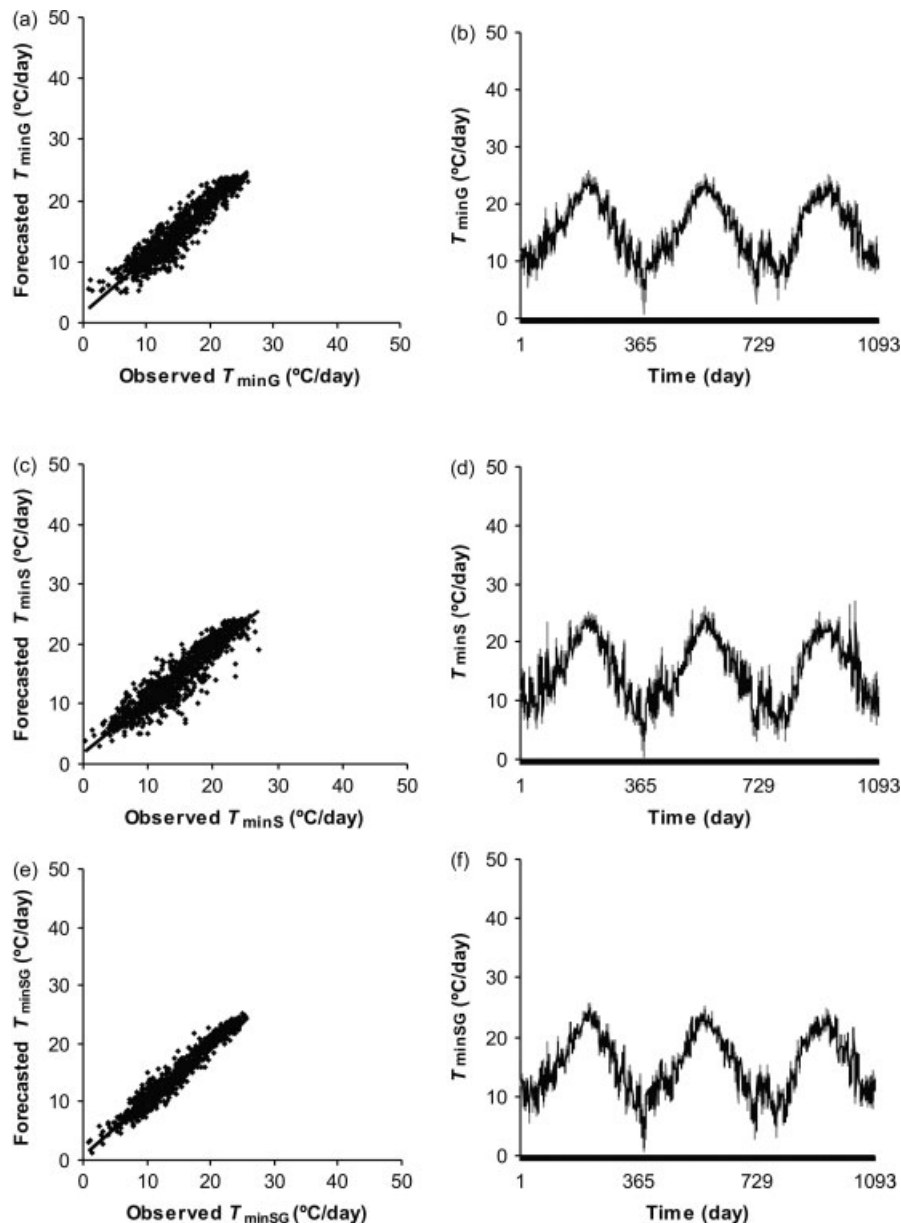


Figure 9. Forecasting daily minimum temperature time series by RBF method in scatter graphic *versus* line graphic (a) and (b) for Geyve ( $T_{\min G}$ ), (c) and (d) for Sakarya ( $T_{\min S}$ ), (e) and (f) for neighbouring station ( $T_{\min SG}$ ).  $y$  is the equation used for forecast and  $R$  is the correlation coefficient between observed and forecasted values in graphics (a), (c) and (e). The grey line is the observed value; the black line is the forecasted value in graphics (b), (d) and (f). (a)  $y = 0.8915x + 2.5169$   $R^2 = 0.950$ ; (c)  $y = 0.873x + 2.4035$   $R^2 = 0.942$ ; (e)  $y = 0.9558x + 1.1371$   $R^2 = 0.980$ .

method provided superior performance in predicting  $R$  (Figure 7). That is why they are plotted in scatter and line graphics. Both graphics represent the values of the forecasted and observed temperature values in the time series for the testing period.

The FFBP and the RBF methods performed quite well providing good agreement with the estimates compared with the GRNN and the MLR methods in daily maximum temperature ( $T_{\max}$ ) forecasting in terms of the selected performance criteria, RMSE,  $R$  and IA. While forecasting daily maximum temperature, the RBF simulations give the best results (Figure 8).

In the daily minimum temperature ( $T_{\min}$ ) forecasting, on the other hand, the FFBP and the RBF methods had superior performance compared with the GRNN and the

MLR methods, in terms of the selected performance criteria, RMSE and IA. The RBF method had the best  $R$  among all methods for the testing period. Again, the RBF simulations give the best results, and its performance is shown in Figure 9.

The employment of the RBF and the GRNN methods has advantages over the FFBP method. First, different performance criteria have been obtained for different the FFBP simulations for the same network configuration due to the random assignment of initial weight values before each simulation. Therefore, a number of simulation steps are needed in order to obtain the best the FFBP performances; in contrast, the RBF and the GRNN methods provide estimations with a unique simulation. The FFBP simulations have been found to be sensitive to the

randomly assigned initial values of correlation weights. This problem, however, has not occurred in the RBF and the GRNN simulations. Lastly, the computational cost of the RBF and the GRNN simulations was greater than that of the FFBP method. Since the periodicity index highly affects the cycle of a time series, its inclusion was beneficial in the current simulations.

Inclusion of the data from the neighbouring station noticeably improved the forecast results. Forecast of  $T_{\text{mean}}$ ,  $T_{\text{max}}$ ,  $T_{\text{min}}$  values for Geyve using the  $T_{\text{mean}}$ ,  $T_{\text{max}}$ ,  $T_{\text{min}}$  values for Sakarya and the past  $T_{\text{mean}}$ ,  $T_{\text{max}}$ ,  $T_{\text{min}}$  values for Geyve provided superior performance criteria compared with the case where only the past Geyve  $T_{\text{mean}}$ ,  $T_{\text{max}}$ ,  $T_{\text{min}}$  were employed. In these methods and data, the RBF simulations provided good agreement for the prediction of ' $T_{\text{mean}}$ ' in terms of the selected performance criteria; RMSE,  $R$  and IA.

Forecast  $T_{\text{mean}}$  provided the highest  $R$ , IA and the lowest RMSE values for both stations compared with  $T_{\text{max}}$  and  $T_{\text{min}}$ . This may be explained with the higher auto-correlation values of  $T_{\text{mean}}$  compared with the other two temperature statistics. Neural network and regression models performed similarly for prediction  $T_{\text{mean}}$ ,  $T_{\text{max}}$  and  $T_{\text{min}}$ , however, the ANN model performance criteria were slightly superior to the MLR models. Although all the ANN methods provided close results in temperature estimation study, the RBF method was found slightly superior compared to other two ANN methods. Therefore only the results of the RBF simulations are plotted in the figures. The performance evaluation criteria values for all methods, however, are presented in Table V and Figure 6.

The reason why the four different techniques employed provided similar results is related to the characteristics of temperature time series used. The temperature time series demonstrates lower variation with respect to other climatic parameters (for example, rainfall and wind). The coefficient of variation of the temperature time series is low except in winter months [December, January and February (Table II)]. This is related to the intense transfer of the various air masses and the movement of cyclones during the winter months. On the annual basis, however, the coefficient of variation values are quite low, i.e. 4.9 and 4.8% for Geyve and Sakarya stations, respectively (Table II).

This low variability of the temperature data is one of the explanations of quite high correlation coefficient ( $R$ ), and quite low RMSE values for the testing periods of the four employed methods (Table V, Figure 6). As a result all four methods provided close and satisfactory results for the estimation of the maximum, mean and minimum temperature series (Table V, Figure 6). Another explanation is the quite low skewness  $c_{\text{sx}}$ , values of the mean, maximum and minimum temperature time series (Table I). The skewness values are close to zero indicating a Gaussian type of probability distribution (normal distribution). It is well known that the MLR assumes normal distribution for the time series analysed. Consequently the regression results are satisfactory for normally

distributed time series, which is the case in the presented study, whereas it is the opposite for the highly skewed time series. In the literature, the ANN methods provided quite superior performances to conventional regression (Cigizoglu, 2003a, 2004; Freiwan and Cigizoglu, 2005) for the hydro meteorological time series having high coefficient variation and skewness values.

It can be concluded that the ANN methods employed in this study are found quite reliable in the temperature estimation study. The applicability of the employed the ANN methods also in the long range temperature forecasting could be analysed in a future study. It is hoped that the presented study can shed light to future ANN studies modelling temperature time series.

### Acknowledgements

The authors would like to thank for partial supports of ITU (Istanbul Technical University) – Scientific Research Program and TUBITAK (Turkish Science and Technological Research Council).

### References

- Alp M, Cigizoglu HK. 2007. Suspended sediment load simulation by two artificial neural network methods using hydro meteorological data. *Environmental Modelling & Software* **22**(1): 2–13.
- ASCE (Task Committee on Application of Artificial Neural Networks in Hydrology). 2000. Artificial neural networks in hydrology. II: Hydrologic application. *Journal of Hydrologic Engineering*, ASCE **5**(2): 124–137.
- Brikundavyi S, Labib R, Trung HT, Rousselle J. 2002. Performance of neural networks in daily streamflow forecasting. *Journal of Hydrologic Engineering* **7**(5): 392–398.
- Broomhead DS, Lowe D. 1988. Multivariable functional interpolation and adaptive networks. *Complex Systems* **2**: 321–355.
- Bryant S, Shreeve TG. 2002. The use of artificial neural networks in ecological analysis: estimating microhabitat temperature. *Ecological Entomology* **27**: 424–432.
- Cavazos T. 1997. Downscaling large-scale circulation to local winter rainfall in North-eastern Mexico. *International Journal of Climatology* **17**: 1069–1082.
- Cigizoglu HK. 2003a. Estimation, forecasting and extrapolation of river flows by artificial neural networks. *Hydrological Sciences Journal-Journal Des Sciences Hydrologiques* **48**(3): 349–361.
- Cigizoglu HK. 2003b. Incorporation of ARMA models into flow forecasting by artificial neural networks. *Environmetrics* **14**: 417–427.
- Cigizoglu HK. 2004. Estimation and forecasting of daily suspended sediment data by multi-layer perceptions. *Advances in Water Resources* **27**: 185–195.
- Cigizoglu HK. 2005a. Generalized regression neural network in monthly flow forecasting. *Civil Engineering and Environmental Systems* **22**: 71–84.
- Cigizoglu HK. 2005b. Application of the generalized regression neural networks to intermittent flow forecasting and estimation. *ASCE, Journal of Hydrologic Engineering* **10**(4): 336–341.
- Cigizoglu HK, Alp M. 2006. Generalized regression neural network in modelling river sediment yield. *Advances in Engineering Software* **37**: 3763–3768.
- Cigizoglu HK, Kisi O. 2006. Methods to improve the neural network performance in suspended sediment estimation. *Journal of Hydrology* **317**: 221–238.
- Crane RG, Hewitson BC. 1998. Doubled CO<sub>2</sub> climate change scenarios for the Susquehanna Basin: Down-scaling from the genesis general circulation model. *International Journal of Climatology* **18**: 65–76.
- Dibike YB, Coulibaly P. 2006. Temporal neural networks for downscaling climate variability and extremes. *Neural Network* **19**: 135–144.
- Elsner JB, Tsonis AA. 1992. Nonlinear prediction, chaos, and noise. *Bulletin of the American Meteorological Society* **73**: 49–60.

- Erinc S. 1957. *Applied Climatology and Climatic Conditions of Turkey*. Istanbul Technical University, Hydrogeology Institute Publication: Istanbul, [In Turkish].
- Freiwan M, Cigizoglu HK. 2005. Prediction of total monthly rainfall in Jordan using feed forward back propagation method. *Fresenius Environmental Bulletin* **14**(2): 142–151.
- Gardner MW, Dorling SR. 1998. Artificial neural networks (the multilayer perceptron) a review of applications in the atmospheric sciences. *Atmospheric Environment* **6**(32): 2627–2636.
- Gardner MW, Dorling SR. 2000. Statistical surface ozone models: an improved methodology to account for non-linear behaviour. *Atmospheric Environment* **34**: 21–34.
- Hewitson BC, Crane RG. 1992. Large-scale atmospheric controls on local precipitation in tropical Mexico. *Geophysical Research Letters* **19**: 1835–1838.
- Hewitson BC, Crane RG. 1996. Climate downscaling: techniques and application. *Climate Research* **7**: 85–95.
- Holder L. 1985. *Multiple Regression in Hydrology*. Institute of Hydrology Press: Wallingford, CT.
- Ikiel C. 2005. Rainfall regime regions in Turkey (a statistical climate study). In *International Conference on Forest Impact on Hydrological Process and Soil Erosion*, Sofia, Yundola, 5–8 October, 2005.
- IPCC (Intergovernmental Panel on Climate Change). 2007. Climate Change 2007: The Physical Science Basis, Summary for Policymakers, (published online 2 Feb 2007 at <http://www.ipcc.ch/>).
- Jang JD, Viau AA. 2004. Neural network estimation of air temperatures from AVHRR Data. *International Journal of Remote Sensing* **25**: 4541–4554.
- Jorquera H, Pérez R, Cipriano A, Espejo A, Letelier MV, Acuna G. 1998. Forecasting ozone daily maximum levels at Santiago, Chile. *Atmospheric Environment* **32**: 3415–3424.
- Kaymaz B. 2005. Hazards and their impact on human. 29. *IMISE (International Movement for Interdisciplinary Study of Estrangement) Conference*. The American University of Paris: Paris, 4–9 July, 2005.
- Kaymaz B, Ikiel C. 2004. The effects of climatic conditions on fruit production in Geyve. *International Symposium on Earth System Science (ISES)*, Istanbul University: Istanbul, 8–10 September, 2004.
- Kindap T, Unal A, Chen SH, Hu Y, Omdan MT, Karaca M. 2006. Long range aerosol transport from Europe to Istanbul, Turkey. *Atmospheric Environment* **40**: 3536–3547.
- Kuligowski RJ, Barros A. 1998. Experiments in short-term precipitation forecasting using artificial neural networks. *Monthly Weather Review* **126**: 470–482.
- Maier H, Dandy G. 2000. Neural networks for the predictions and forecasting of water resources variables: Review of modeling issues and applications. *Environmental Modelling & Software* **15**: 101–124.
- Makarynskyy O, Makarynska D, Kuhn M, Featherstone WE. 2004. Predict sea level variations with artificial neural networks at Hillarys boat harbour, Western Australia. *Estuarine Coastal and Shelf Science* **61**: 351–360.
- Mihalakakou G, Santamouris M, Asimakopoulos D. 1998. Modeling ambient air temperature time series using neural networks. *Journal of Geophysical Research* **103**: 509–517.
- Ramirez MCV, Velhob HFC, Ferreira NJ. 2005. Artificial neural network technique for rainfall forecasting applied to the São Paulo region. *Journal of Hydrology* **301**: 146–162.
- Schoof JT, Pryor SC. 2001. Downscaling temperature and precipitation: a comparison of regression-based methods and artificial neural networks. *International Journal of Climatology* **21**: 773–779.
- Smith BA, Mcclendon RW, Hoogenboom G. 2005. An enhanced artificial neural network for air temperature prediction. *Transactions on Engineering, Computing and Technology* **7**: 7–12.
- Smith BA, Mcclendon RW, Hoogenboom G. 2006. Improving air temperature prediction with artificial neural networks. *International Journal of Computational Intelligence* **3**: 180–186.
- Specht DF. 1991. A general regression neural network. *IEEE Transactions on Neural Networks* **2**(6): 568–576.
- Tang B, Flato GM, Greg H. 1994. A study of arctic ice and sea level pressure using pop and neural network models. *Atmosphere-Ocean* **32**(3): 507–529.
- Tangang FT, Tang B, Monaham AH, Hsieh WW. 1998. Forecasting ENSO events: a neural network-extended EOF approach. *Journal of Climate* **11**: 29–41.
- Thirumalaiah K, Deo MC. 1998. River stage forecasting using artificial neural networks. *Journal of Hydrologic Engineering* **3**(1): 26–32.
- Thirumalaiah K, Deo MC. 2000. Hydrological forecasting using artificial neural networks. *Journal of Hydrologic Engineering* **5**(2): 180–189.
- TMARA (The Turkish Ministry of Agriculture and Rural Affairs). 2005. Agriculture Provincial Directorate of Sakarya, Agricultural Crop Records.
- Trigo RM, Palutikof JP. 1999. Simulation of daily temperatures for climate change scenarios over Portugal: a neural network model approach. *Climate Research* **13**: 45–59.
- Unal Y, Kindap T, Karaca M. 2003. Redefining climate zones for Turkey using cluster analysis. *International Journal of Climatology* **23**: 1045–1055.
- Zhigang Y, Hongbin C, Longfu L. 2005. Retrieving atmospheric temperature profiles from AMSU-A data with neural networks. *Advances in Atmospheric Sciences* **22**: 606–616.
- Zwiers FW, Storch HV. 2004. On the role of statistics in climate research. *International Journal of Climatology* **24**: 665–680.